

Practical Implementation of Lattice QCD Simulation on Intel Xeon Phi Knights Landing

Issaku Kanamori
Department of Physics,
Hiroshima University
Higashi-hiroshima 739-8526, Japan
Email: kanamori@hiroshima-u.ac.jp

Hideo Matsufuru
Computing Research Center,
High Energy Accelerator Research Organization (KEK)
Oho 1-1, Tsukuba 305-0801, Japan
Email: hideo.matsufuru@kek.jp

Abstract—We investigate implementation of lattice Quantum Chromodynamics (QCD) code on the Intel Xeon Phi Knights Landing (KNL). The most time consuming part of the numerical simulations of lattice QCD is a solver of linear equation for a large sparse matrix that represents the strong interaction among quarks. To establish widely applicable prescriptions, we examine rather general methods for the SIMD architecture of KNL, such as using intrinsics and manual prefetching, to the matrix multiplication and iterative solver algorithms. Based on the performance measured on the Oakforest-PACS system, we discuss the performance tuning on KNL as well as the code design for facilitating such tuning on SIMD architecture and massively parallel machines.

I. INTRODUCTION

Quantum Chromodynamics (QCD) is the fundamental theory of the strong interaction among quarks. Despite its essential roles in the elementary particle physics, the lack of analytical method to treat its large coupling at low energy (equivalently at long distance) prevents us from solving QCD in general. The lattice QCD, that is formulated on a 4-dimensional Euclidean lattice, enables us to tackle such problems by numerical simulations [1]. Quantifying with the path integral formalism, the theory resembles a statistical mechanical system to which the Monte Carlo methods apply. Typically the most time consuming part of the lattice QCD simulations is solving a linear equation for a large sparse fermion matrix that represents the interaction among quarks. As the lattice size becomes large necessarily to precision calculation, the numerical cost grows rapidly. The lattice QCD simulations have been a typical problem in high performance computing and conducted development of supercomputers such as QCDPAX [3] and QCDOC [4].

There are two distinct trends in high performance machines. One is accelerators, represented by GPUs, which is composed of many cores of $O(1000)$. The Intel Xeon Phi architecture is a variant of the other type, massively parallel clusters, while it has potential to work as an accelerator. Knights Landing (KNL), the second generation of Xeon Phi series, reinforced

usability as a massive parallel machine. Its performance is assured by the SIMD architecture. Elaborated assignments of vector registers and exploiting SIMD instructions are essential to achieve desired performance.

In this paper, we port a lattice QCD simulation code to Intel Xeon Phi Knights Landing. The aim of this work is not a state-of-the-art tuning on KNL, but to establish prescriptions that are applicable to wide part of the application with practical performance. While a hot spot of the QCD simulation tends to concentrate in small part of programs, there are plenty amount of code for measuring various physical quantities that have been accumulated in legacy codes. One frequently needs to accelerate such a code on a new architecture. Thus it is important to establish simple procedures to achieve acceptable performance as well as implication to future development of code. For this reason, we restrict ourselves in rather general methods: change of data layout, application of Intel AVX-512 intrinsics and prefetching. As a testbed of our analysis, we choose two types of fermion matrices that are widely used together with iterative linear equation solver algorithms.

This paper is organized as follows. The next section briefly introduce the linear equation system in lattice QCD simulations with fermion matrices employed in this work. Features of KNL architecture are summarized in Section III. Section IV describes the details of our implementation. In the following sections, we measure the performance of individual fermion matrices and the whole linear equation solvers. The last section discusses implication of our results.

II. LATTICE QCD SIMULATION

A. Structure of lattice QCD simulation

For the formulation of lattice QCD and the principle of the numerical simulation, there are many textbooks and reviews [1]. Thus we concentrate on the linear equation system for the fermion matrix, to which high computational cost is required.

The lattice QCD theory consists of fermion (quark) fields and a gauge (gluon) field. The latter mediates interaction among quarks and are represented by ‘link variables’, $U_\mu(x) \in SU(3)$, where $x = (x_1, x_2, x_3, x_4)$ stands for a lattice site and $\mu=1-4$ is the spacetime direction. In numerical simulations the lattice size is finite, $x_\mu = 1, 2, \dots, L_\mu$. The fermion field is represented as a complex vector on lattice

Submitted to LHAM’17 “5th International Workshop on Legacy HPC Application Migration” in CANDAR’17 “The Fifth International Symposium on Computing and Networking” and to appear in the proceedings.

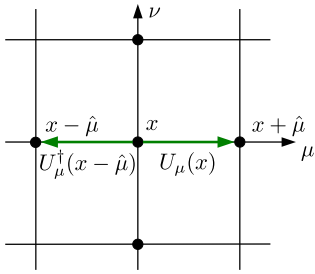


Fig. 1. The schematic feature of the Wilson fermion matrix.

sites, which carries 3 components of ‘color’ and 4 components of ‘spinor’, thus in total 12, degrees of freedom on each site. The dynamics of fermion is governed by a functional $S_F = \sum_{x,y} \psi^\dagger(x) D[U]^{-1}(x,y) \psi(y)$, where $D[U]$ is a fermion matrix. A Monte Carlo algorithm is applied to generate an ensemble of the gauge field $\{U_\mu(x)\}$, that requires to solve a linear equation $x = D^{-1}\psi$ many times.

B. Fermion matrix

There is a variety of the fermion operator $D[U]$, since its requirement is to coincide with that of QCD in the continuum limit, the lattice spacing $a \rightarrow 0$. Each formulation has advantages and disadvantages. As a common feature, the matrix is sparse because of the locality of the interaction. In this paper, we examine the following two types of fermion matrices.

1) *Wilson fermion matrix*: The first one called the Wilson fermion matrix has the form

$$D_W(x,y) = (m_0 + 4)\delta_{x,y} - \frac{1}{2} \sum_{\mu=1}^4 [(1 - \gamma_\mu)U_\mu(x)\delta_{x+\hat{\mu},y} + (1 + \gamma_\mu)U_\mu^\dagger(x - \hat{\mu})\delta_{x-\hat{\mu},y}], \quad (1)$$

where x, y are lattice sites, $\hat{\mu}$ the unit vector along μ -th axis, and m_0 the quark mass. Fig. 1 indicates how the interaction to the neighboring sites are involved in the matrix. As mentioned above, the link variable $U_\mu(x)$ is a 3×3 complex matrix acting on color and γ_μ is a 4×4 matrix acting on the spinor degrees of freedom. Thus D_W is a complex matrix of the rank $4N_c L_x L_y L_z L_t$. It is standard to impose the periodic or antiperiodic boundary conditions.

2) *Domain-wall fermion matrix*: The second fermion matrix we treat is called the domain-wall fermion. This matrix D_{DW} is defined by extending the spacetime to a 5-dimensional lattice. The structure of D_{DW} in the 5th direction reads

$$D_{DW} = \begin{pmatrix} D_W + 1 & -P_- & 0 & \cdots & mP_+ \\ -P_+ & D_W + 1 & -P_- & & 0 \\ 0 & -P_+ & D_W + 1 & \ddots & \vdots \\ \vdots & & \ddots & \ddots & -P_- \\ mP_- & 0 & \cdots & -P_+ & D_W + 1 \end{pmatrix}, \quad (2)$$

where $D_W(x,y)$ is the Wilson fermion matrix above (with m_0 set to certain value), and m instead represents the quark mass. P_\pm are 4×4 matrices acting on the spinor components. The size of the 5th direction, N_s , is also a parameter of D_{DW} . Eq. (2) means that D_{DW} is a block tridiagonal matrix

TABLE I

FEATURES OF FERMION MATRICES: THE NUMBER OF FLOATING POINT OPERATION AND THE DATA TRANSFER BETWEEN MEMORY AND PROCESSOR PER SITE. FOR THE DOMAIN-WALL MATRIX, THE 5TH DIRECTIONAL SIZE IS SET AS $N_s = 8$.

Fermion type	N_{flop}/site	data/site [B] (float)	Byte/Flop
Wilson	1368	1536 B	1.12
Domain-wall	11520	8256 B	0.72

including the boundary components in the fifth direction. Note that $U_\mu(x)$ is common in the 5th direction. The domain-wall fermion is widely used because of its good theoretical properties despite larger numerical cost than the Wilson matrix.

There are several possible ways to implement D_{DW} . The simplest way is to repeatedly use the implementation of D_W to a set of 4-dimensional vectors. Another way is to treat the structure in the 5th direction as additional internal degrees of freedom, together with the color and spinor ones. The latter has an advantage in cache reuse. We compare the both implementation and found that the latter achieves better performance, and thus concentrate on it in the following.

3) *Features of the fermion matrices*: Although these fermion matrices share the property of locality and sparseness, they have different features in data size transferred between the memory and the processor cores, number of arithmetic operations, and data size of communication to other MPI process. Table I summarizes the former two values per site for single precision data. For the domain-wall fermion matrix, these numbers depend on the size of 5th direction, N_s . Hereafter we adopt $N_s = 8$ as a typical example. As quoted in Table I, the domain-wall matrix tends to have smaller byte-per-flop value, due to the independence of the link variable $U_\mu(x)$ in the 5th direction.

C. Linear equation solver

Since the fermion matrices are large and sparse, iterative solvers based on the Krylov subspace method are widely used. For the Wilson fermion matrix, we employ the BiCGStab algorithm for a nonhermitian matrix. As for the domain-wall fermion, BiCGStab algorithm does not work because its eigenvalues scatter also in the left side of the imaginary axis. We thus apply the conjugate gradient (CG) algorithm to a hermitian positive matrix $D_{DW}^\dagger D_{DW}$.

In practice a mixed precision solver is applicable. In this case the single precision solver applied as the inner solver determines the performance. Therefore we measure the performance with the single precision. While there are variety of improvement techniques for a large-scale linear systems, such as a multi-grid or domain-decomposition methods, they are beyond the scope of this paper.

III. KNIGHTS LANDING ARCHITECTURE

The Knights Landing is the second generation of Intel Xeon Phi architecture, whose details are found in [2]. Its maximal peak performance is 3 and 6 TFlops for double and single precision, respectively. It is composed of maximally 72 cores,

in units of a tile containing two cores. Each tile has distributed L2 cache that is shared with 2 cores. In addition to DDR4 with about 90 GB/s, MCDRAM of maximally 16 GB accessible with 400 GB/s is available with one of three modes: cache, flat, and hybrid. Each core supports 4-way hyperthreading. The SIMD instruction AVX-512 is available. 32 vector registers of 512-bit length are assigned to 8 double or 16 single precision numbers.

Our target machine is the Oakforest-PACS system hosted by Joint Center for Advances High Performance Computing (JCAHPC, University of Tokyo and University of Tsukuba) [5]. The system is composed of 8208 nodes of Intel Xeon Phi 7250 (68 cores, 1.4 GHz) connected by full-bisection fat tree network of the Intel Omni-Path interconnect. It has 25 PFlops of peak performance in total, and started public service in April 2017.

IV. IMPLEMENTATION

A. Simulation code

As the base code, we choose the Bridge++ code set [6], [7], which is described in C++ with the object-oriented design. This code set allows us to replace fermion matrices and solver algorithms independently. Porting of Bridge++ to accelerators are performed in [8]. In the original Bridge++, hereafter called the Bridge++ core library, the data is in double precision and in fixed data layout. Following the strategy employed in [8], we extend the vectors and matrices so as to enable any data layout and changing the data type. From the core library, the linear equation solver is offloaded to the newly developed code. This enables us to tune the hot spot on the specific architecture with keeping the remaining part of Bridge++ available. Following the implementation of Bridge++, we parallelized the code with MPI and employ OpenMP for multi-threading.

B. Related works

Since the lattice QCD simulation, in particular the fermion matrix multiplication, is considered a typical problem of high performance computing, it is examined in a textbook of KNL [2]. Its chapter 26 is devoted to performance tuning of the Wilson-Dslash operator, corresponding to the Wilson matrix above, using the QPhiX library [9]. On a single KNL with 68 cores at 1.4 GHz, the maximal performance of the Wilson matrix multiplication achieved 272 and 587 GFlops for double and single precision, respectively.

As for the first generation of Xeon Phi, Knights Corner, there are several works [10], [11], [12], [13], [14], [15], [16]. Joo *et al.* [10] is the direct base of the QPhiX library on KNL. Ref. [14] developed a library named ‘Grid’ for the SIMD architecture, and has largely affected our work. These works would be extended to the KNL as well.

C. Implementation

To fully exploit the SIMD architecture of KNL, rearrangement of data is inevitably important. For double and single precision data types, 512-bit register corresponds to 8 and 16 floating point numbers, respectively, so we rearrange the

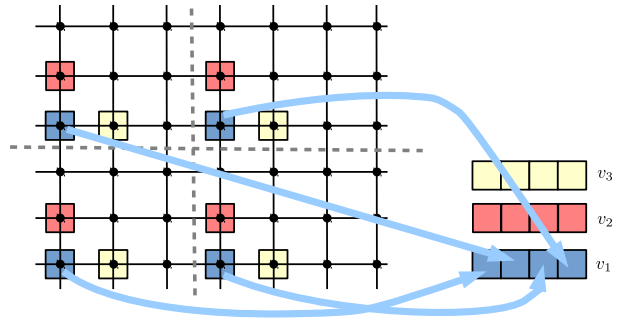


Fig. 2. The site index ordering. For float type complex variables, we use 3 dimensional analogues of this figure.

date in these units. We implement the code in C++ template classes and instantiate them for double and float data types individually. Since the vector data in lattice QCD are complex, there are several possibilities for the ordering of real and imaginary parts. Considering the number of SIMD registers and the number of the degree of freedom on each site, we decide to place the real and imaginary parts as consecutive data on the memory. The color and spinor components are distributed to separate registers. For float type, data on eight sites are packed into a single register and processed simultaneously.

There is flexibility how to fold lattice sites into the data array. We have tested several reasonable types of site ordering for the Wilson fermion matrix and found similar performance. Throughout this paper, we adopt one of them in which the implementation has been made most progress. This site ordering is introduced in [14]. Fig. 2 displays how the index of site is folded into SIMD-vector data. This indexing does not require shuffling inside the vector variables during the stencil calculation except for the boundary sites in a local process, which makes the implementation easy. It also allows us a flexible choice of local lattice volume. In our implementation, local lattice sizes in y -, z -, and t -directions must be even to pack 8 complex numbers into a single SIMD-vector. A possible disadvantage is a load imbalance between bulk and boundary sites. In most cases, however, this is hidden in the larger imbalance due to packing and unpacking of the data for MPI communication.

D. Tuning procedure

1) *Data alignment*: For a better performance with SIMD-vector data, the data must be aligned by 64 bytes (*i.e.* 512 bits) in AVX512 architecture. To allocate the data, we use `std::vector` in the standard C++ template library with providing an aligned allocator. This allocation is done when only the master thread is working. The use of `std::vector` ensures that the data are allocated on contiguous area of the memory. For the KNL architecture, this may cause imbalance of affinity between cores and memory and decrease of performance in particular with large number of cores per process. We nonetheless adopt this setup because of the least modification of previously developed codes.

2) *Using Intrinsics*: The arithmetics for the SIMD-vector variables are implemented with intrinsics. For example, the following code is an implementation of complex multiplication $a * b$ using AVX-512 intrinsics.

```
// a, b are vector variables
__m512 a_r=_mm512_moveldup_ps(a);
__m512 a_i=_mm512_movehdup_ps(a);
__m512 bt=_mm512_permute_ps(b,0xB1);
a_i=_mm512_mul_ps(a_i, bt);
__m512 c=_mm512_fmaddsub_ps(a_r,b,a_i);
```

One can incorporate such codes with intrinsics by making use of inline functions, C++ templates, or preprocessor macros.

We instead make use of `simd` directory in the ‘Grid’ library [14], where a wrapper to the vector variable (`__m512`) and complex arithmetics are defined by using the intrinsics. Using a template class defined there, operation $a * b$ can be written such as `vComplexF c=a*b`.

3) *Prefetching*: We compare the manual prefetch and the automated prefetch by compiler. The most outer loop of the matrix is in the site index. At each site, we accumulate 8 stencil contributions, from $+x, -x, \dots, -t$ directions in order. The prefetch to L1 and L2 cache is inserted 1 and 3 steps before the computation, respectively. That is, before accumulating a $(+x)$ -contribution, data needed for $(-x)$ -contribution is prefetched to the L1 cache and $(-y)$ -contribution is to the L2 cache. We use `__mm_prefetch` with `__MM_HINT_T0` and `__MM_HINT_T1` to generate the prefetch order. The following is a pseudo code to show the prefetch insertions:

```
for(s=0; s<num_of_sites; s++){
#pragma noprefetch
// +x
prefetch_to_L1(-x);
prefetch_to_L2(-y);
accumulate_from(+x);
// -x
prefetch_to_L1(+y);
prefetch_to_L2(+z);
accumulate_from(-x);
...
}
```

It is not straightforward to insert prefetch commands appropriately. One needs to tune the variables and the place to insert referring to a profiler, *e.g.* Intel Vtune amplifier. The performance may sensitive to the problem size, choice of parameters such as the number of threads, and so on.

4) *Thread task assignment*: Since the lattice extends over the machine nodes, the matrix and the reduction of vectors require communication among nodes. The function of matrix processes the following steps in order: (1) Packing of the boundary data for communication, (2-a) Doing communication, (2-b) Operations of the bulk part, and (3) Unpacking the boundary data. (2-a) and (2-b) can be overlapped, and how efficient is this is important for the total performance.

We restrict ourselves in the case that only the master thread performs the communication, *i.e.* corresponding to `MPI_THREAD_FUNNELED`. For the implementation of the steps (2-a) and (2-b) above, there are two possibilities: (i)

arithmetic operational tasks are equally assigned to all the available threads, and (ii) the master thread concentrates the communication and other threads bear the arithmetic tasks. In this work, we adopt the case (ii).

V. PERFORMANCE OF WILSON FERMION MATRIX

A. Machine environment

The performance is measured on the Oakforest-PACS system. We use the Intel compiler of version 17.0.4 with options `-O3 -ipo -no-prec-div -xMIC-AVX512`. On execution, we use job classes with the cache mode of MCDRAM. According to the tuning-guide provided by JCAHPC, we adopt the following setup. To avoid OS jitter, the 0th and 1st cores on each KNL card are not assigned for execution. `KMP_AFFINITY=compact` is set if more than 1 thread is assigned to a core (unset for 1 thread/core).

B. Wilson fermion matrix

1) *Task assignment to threads*: We start with the Wilson fermion matrix. We first compare the performance for combinations of a number of cores per MPI process and a number of threads per core. For the former, (1) one core per process, (2) two cores (one tile) per process, and (3) 64 cores (whole KNL card) per process. For the latter, making use of the hyperthreading, the following three cases are examined: (a) one thread per core, (b) two threads per core, and (c) four threads per core. The actual number of threads per MPI process is multiple of numbers of cores and threads per core.

We compare one, two, and four threads per core cases. Fig. 3 shows the results with 1-node and 16-node, generated with the strong scaling on $32^3 \times 64$ lattice. For the case (3), copy of the boundaries is enforced so as to compare with the other cases on the same footing. For the case (1) and (2), dependence on the number of threads per core is not strong. Including the cases of other numbers of nodes, there is a tendency of achieving the best performance with 2 threads per MPI process for case (1) and (2), and 1 thread per core for case (3).

2) *Prefetching*: Effect of manual prefetch against the automated prefetch by compiler is displayed in Fig. 4. In the single node case, where no inter-node communication is needed, the manual prefetch improves the performance by more than 20%. Contrary to a statement in [2], manual prefetching is effective to our case. Increasing the number of nodes, however, the effect is gradually washed and becomes a few percent at 16 nodes as shown in Fig. 4. Since our target lattice sizes assumes more than $O(10)$ KNL nodes, the advantage of manual prefetch is not manifest compared to involved tuning effort. For this reason, we do not apply it to the linear algebraic functions and the domain-wall fermion matrix, while the following measurement of the Wilson matrix is done with the tuned code.

Here we summarize the output of Intel Vtune Amplifier for the Wilson matrix multiplication with a single process of 64 threads. Applying the manual prefetch, L2 cache hit rate increases from 76.7% to 99.1%. With the manual prefetch, the UTLB overhead and the page walk are 0.0% and 0.2%

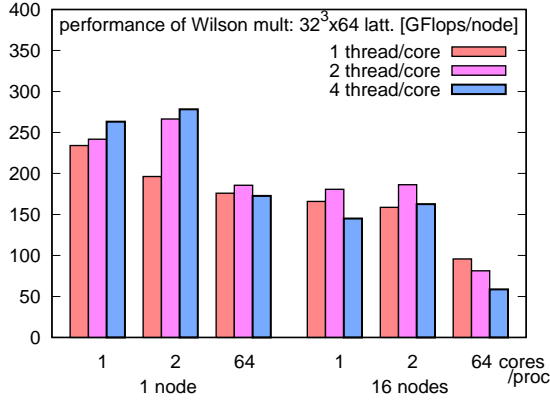


Fig. 3. Comparison of numbers of threads per core.

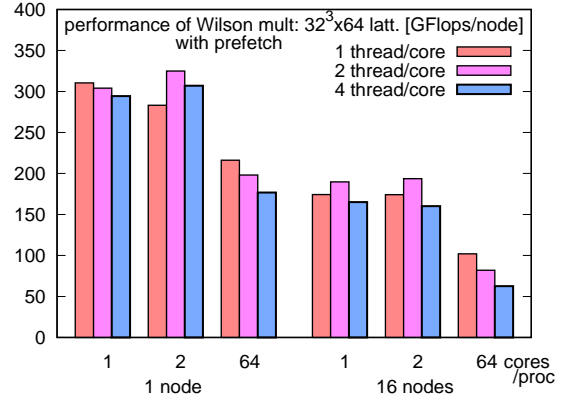


Fig. 4. Effect of manual prefetching. The performance of the Wilson matrix multiplication is measured on a $32^3 \times 64$ lattice.

of clockticks, respectively. The metric SIMD Compute-to-L2 Access Ratio reaches as large as 2,023. For the whole BiCGStab solver examined below, however, the L2 hit rate decreases to 84.4%, as explained by the larger byte-per-flop rate of the solver algorithm.

3) *Comparison to other codes*: Now we compare the performance of the Wilson matrix multiplication to other codes under the condition of a single process on a single KNL. As quoted already, QPhiX library achieves 587 GFlops for single precision [2] on a $32^3 \times 96$ lattice. The GRID library [14] provides a benchmark of the Wilson matrix that we run on the same environment as this work. On $32^3 \times 64$ lattice, based on v0.7.0, it gives the best performance with one thread/core and amounts to 348.6 GFlops that is comparable to our result. While our result is not as fast as QPhiX, it shows that large fraction of performance can be achieved with widely applicable techniques. These values are reasonable considering the memory bandwidth of MCDRAM and the byte-per-flop in Table I, while far below the peak performance.

For reference, we also measure the performance of the original Bridge++, that is implemented in not SIMD-oriented manner and only in the double precision. The best performance is obtained with 4 threads/core and results in 60.0 GFlops, which roughly corresponds to 120 GFlops in single precision. This indicates the impact of the SIMD-oriented tuning.

4) *Scaling property of matrix multiplication*: Now we observe the scaling properties of the Wilson matrix multiplication. In the following, we adopt 1, 2, and 2 threads/core for 64, 2, and 1 cores/process, respectively. The top panel of Fig. 5 shows the weak scaling plot for the $16^3 \times 32$ lattice in each node. In the measurements, we do not enforce the copy of the boundary data unless it is really needed. For reference, if it is enforced on a single node with 64 cores/process, the performance becomes 100.4 and 176.0 GFlops on $16^3 \times 32$ and $32^3 \times 64$ lattices, respectively. For the 64 cores/process on multiple nodes, the performance is about the half of the other two cases. This may be explained by that all the 64 cores in a node share the whole memory of the node so that imbalance of accessibility to the memory among the cores exists. The cases of 1 or 2 cores/process achieve more than 170 GFlops/node

up to 256 nodes.

The bottom panel of Fig. 5 shows the strong scaling on a $32^3 \times 64$ lattice. In this case, as the number of nodes increases, the local lattice volume inside each node decreases so that the communication overhead becomes more and more significant. Again the 64 cores/process case exhibits less performance than other two cases. For the strong scaling, the performance depends on how the lattice is divided into sublattices. We plot several cases at each number of nodes. For the case of 1 and 2 cores/process, the performance at 16 nodes is about 2/3 of that of single node.

C. Performance of BiCGStab solver

For the Wilson matrix, the BiCGStab solver works efficiently. We compose the BiCGStab algorithm with BLAS-like library. For the linear algebraic functions, we apply neither manual prefetch nor additional compiler option for prefetch. While the Wilson matrix part is improved by manual prefetch, this effect is small because the performance is determined by the linear algebraic functions.

The top panel of Fig. 6 shows the weak scaling for the BiCGStab solver on a $16^3 \times 32$ lattice in each node. Because of larger byte-per-flop values of the linear algebraic functions, the performance reduces to about 1/4 of the matrix multiplication at 256 nodes. The difference of 64 cores/process and other two cases also decrease because of the linear algebraic functions. The worse scaling as the number of node is caused by the reduction operations. The bottom panel of Fig. 6 shows the strong scaling plot of the solver on $32^3 \times 64$ lattice. While the difference of 64 cores/process and other two cases shrinks, smaller numbers of cores/process achieve better performance for large number of nodes. In total, these results indicate that small number of cores per MPI process has advantage, if the memory size and the local lattice volume allow.

VI. PERFORMANCE OF DOMAIN-WALL FERMION MATRIX

A. Performance of matrix multiplication

For the domain-wall fermion matrix, the condition of performance measurement is the same as the Wilson matrix

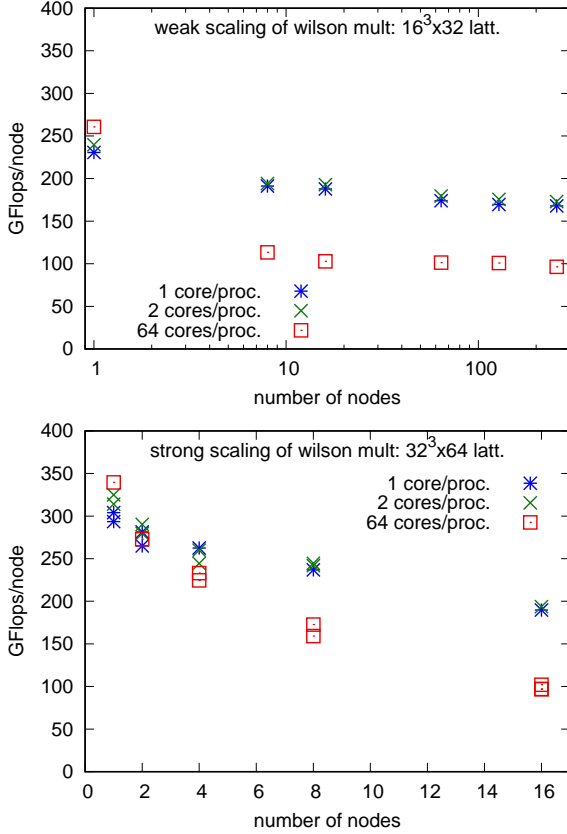


Fig. 5. Scaling plots for the Wilson matrix multiplication. Top: weak scaling with a $16^3 \times 32$ lattice in each node. Bottom: strong scaling with a $32^3 \times 64$ lattice.

except for no manual prefetch is applied. The domain-wall multiplication achieves better performance than the Wilson matrix, as expected from smaller byte-per-flop value due to the reuse of link variable $U_\mu(x)$, as well as the larger number of arithmetic operations per lattice site.

The top panel of Fig. 7 displays a weak scaling plot of the domain-wall matrix multiplication for a $16^3 \times 32$ lattice in each node. On a single node with 64 cores/process, if the boundary data copy is enforced, the performance becomes 155.2 GFlops on a $16^3 \times 32$ lattice and 211.8 GFlops on a $32^3 \times 64$ lattice for the weak and strong scaling, respectively. While the 1 and 2 cores/process cases exhibit good scaling behavior, multi-node result of 64 cores/process is quite bad. What is different from the Wilson matrix is larger size of boundary data transferred at the communication. How such reduction of performance occurs and how can be avoided is now under investigation. The strong scaling on a $32^3 \times 64$ lattice in the bottom panel of Fig. 7 shows similar tendency as the Wilson matrix, except for the reduction of the 64 cores/process data at 16 nodes.

For the 64 cores/process data, we observe large fluctuations up to almost factor 10 in the elapsed time. We have not understood why such fluctuations occur and are investigating the cause. For this reason, we do not include the data for 64 cores/process in the measurement of the CG solver below.

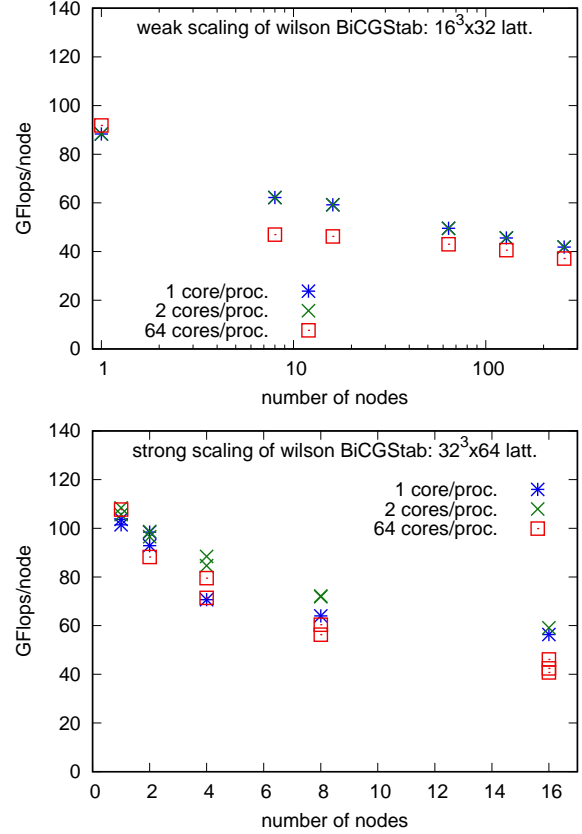


Fig. 6. Scaling property of the BiCGStab solver with Wilson matrix. Top: weak scaling plot for a $16^3 \times 32$ lattice in each node. Bottom: strong scaling on a $32^3 \times 64$ lattice.

B. Performance of CG solver

For the domain-wall fermion, we apply the CG algorithm to the matrix $D^\dagger D$. Fig. 7 displays the weak (top) and strong (bottom) scaling plots for the CG solver. Better scaling behaviors than those of the Wilson matrix are explained by larger weight of the matrix multiplication in the algorithm and larger size of vectors. Even for the strong scaling plot, the performance of 1 and 2 cores/process cases almost unchanged as increasing the number of nodes from 1 to 16.

VII. CONCLUSION

In this paper, we apply rather simple prescription to make use of the SIMD architecture of the Intel Xeon Phi KNL processor to a typical problem in lattice QCD simulation. Aiming at widely applying to existing codes, we examine the rearrangement of data layout and AVX-512 intrinsics to arithmetic operations, and examined the effect of manual prefetching. The former two are inevitable to achieve acceptable performance, compared to the original Bridge++ code. The effect of manual prefetching is more restrictive. It amounts to dedicated efforts only on single node or small number of nodes. Comparing the choices of numbers of cores per MPI process, small numbers of cores per MPI process have advantages as increasing number of nodes.

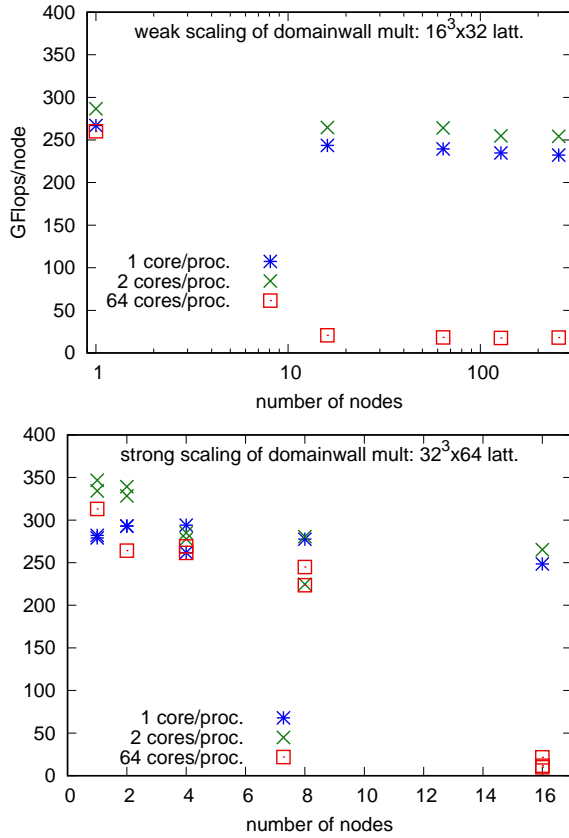


Fig. 7. The weak and strong scaling plots of the domain-wall matrix multiplication. For the weak scaling, $16^3 \times 32$ lattice per node. For the strong scaling, $32^3 \times 64$ lattice.

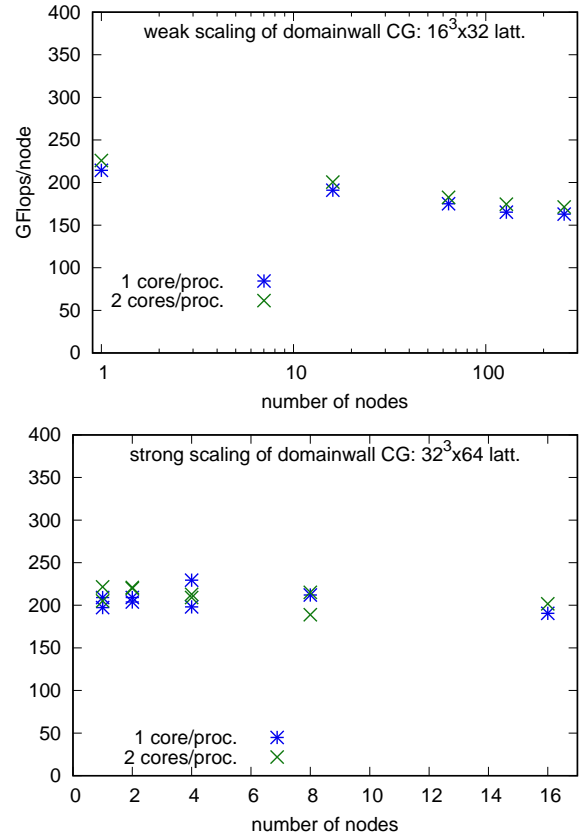


Fig. 8. The weak and strong scaling plot for the CG solver with the domain-wall fermion matrix. For the weak scaling, $16^3 \times 32$ lattice per node. For the strong scaling, $32^3 \times 64$ lattice.

Our results indicate two efficient ways of using KNL. On single KNL, multi-thread application without MPI parallelization may work efficiently. The manual prefetch is worth to try. For a multi-node case, adopting small numbers of cores per MPI process, like a massively parallel machine, one can optimize the number of nodes against a given problem size. As for the code of application, it is essential to employ design that enables flexible rearrangement of data layout and incorporation of intrinsics.

ACKNOWLEDGMENT

The authors would like to thank Peter Boyle, Guido Cossu, Ken-Ichi Ishikawa, Daniel Richtmann, Tilo Wettig, and the members of Bridge++ project for valuable discussion. Numerical simulations were performed on Oakforest-PACS system hosted by JCAHPC, with support of Interdisciplinary Computational Science Program in CCS, University of Tsukuba. This work is supported by JSPS KAKENHI (Grant Numbers JP25400284, JP16H03988), and by Priority Issue 9 to be tackled by Using Post K Computer, and Joint Institute for Computational Fundamental Science (JICFuS).

REFERENCES

[1] For modern textbooks, *e.g.*, T. DeGrand, and C. DeTar, “Lattice Methods for Quantum Chromodynamics” (World Scientific Pub., 2006); C. Gat-

tringer and C. B. Lang, “Quantum Chromodynamics on the Lattice” (Springer, 2010)

[2] J. Jeffers, J. Reinders, A. Sodani, “Intel Xeon Phi Processor High Performance Programming Knights Landing Edition” (Elsevier, 2016).

[3] Y. Iwasaki, T.Hoshino T.Shirakawa Y.Oyanagi T.Kawai “QCDPAX: A parallel computer for lattice QCD simulation”, *Comp. Phys. Commun.* 49, 449 (1988).

[4] P.A. Boyle *et al.*, “QCDOC: A 10 Teraflops Computer for Tightly-Coupled Calculations”, SC '04: Proceedings of the 2004 ACM/IEEE Conference on Supercomputing, DOI: 10.1109/SC.2004.46.

[5] Joint Center for Advanced High Performance Computing (JCAHPC), <https://ofp-www.jcahpc.jp/>.

[6] Bridge++ project, <http://bridge.kek.jp/Lattice-code/>.

[7] S. Ueda *et al.*, “Bridge++: an object-oriented C++ code for lattice simulations” *PoS LATTICE2013*, 412 (2014).

[8] S. Motoki *et al.*, “Development of Lattice QCD Simulation Code Set on Accelerators” *Procedia Computer Science* 29, 1701 (2014). H. Matsufuru *et al.*, “OpenCL vs OpenACC: Lessons from Development of Lattice QCD Simulation Code” *Procedia Computer Science* 51, 1313 (2015).

[9] QPhiX library, <https://github.com/JeffersonLab/qphix>.

[10] B. Joo *et al.*, “Lattice QCD on Intel Xeon Phi Coprocessors” *Supercomputing Vol. 7905 of ser. Lecture Notes in Computer Science* pp 40-54 (2013).

[11] R. Li and S. Gottlieb, “Staggered Dslash Performance on Intel Xeon Phi Architecture,” *PoS LATTICE 2014*, 034 (2015).

[12] S. Heybrock *et al.*, “Lattice QCD with Domain Decomposition on Intel Xeon Phi Co-Processors,” doi:10.1109/SC.2014.11.

[13] P. Arts *et al.*, “QPACE 2 and Domain Decomposition on the Intel Xeon Phi,” *PoS LATTICE 2014*, 021 (2015).

[14] P. A. Boyle, G. Cossu, A. Yamaguchi and A. Portelli, “Grid: A next generation data parallel C++ QCD library,” *PoS LATTICE 2015*, 023 (2016).

- [15] H. Kobayashi, Y. Nakamura, S. Takeda and Y. Kuramashi, "Optimization of Lattice QCD with CG and multi-shift CG on Intel Xeon Phi Coprocessor," PoS LATTICE **2015**, 029 (2016).
- [16] T. Boku *et al.*, "A performance evaluation of CCS QCD Benchmark on the COMA (Intel(R) Xeon PhiTM, KNC) system," PoS LATTICE **2016**, 261 (2016).